Received: 29 May 2018 | Revised: 10 October 2018 | Accepted: 12 November 2018

DOI: 10.4218/etrij.2018-0231

ORIGINAL ARTICLE

WILEY ETRI Journal

Is the SAM phantom conservative for SAR evaluation of all phone designs?

Ae-Kyoung Lee | **Seon-Eui Hong** | **Hyung-Do Choi**

Broadcasting and Media Research Laboratory, Electronics and Telecommunications Research Institute, Daejeon, Rep. of Korea

Correspondence
Ae-Kyoung Lee, Broadcasting and Media Research Laboratory, Electronics and Telecommunications Research Institute, Daejeon, Rep. of Korea.
Email: aklee@etri.re.kr

Funding information
This work was supported by the ICT R&D program of MSIP/IITP, Korea [2017-0-00961, Study on the EMF exposure control in smart society] and [2019-0-00102, A study on public health and safety in a complex EMF environment].

The specific anthropomorphic mannequin (SAM) phantom was designed to provide a conservative estimation of the actual peak spatial specific absorption rate (SAR) of the electromagnetic field radiated from mobile phones. However, most researches on the SAM phantom have been based on early phone models. Therefore, we numerically analyze the SAM phantom to determine whether it is sufficiently conservative for various types of mobile phone models. The peak spatial 1- and 10-g averaged SAR values of the SAM phantom are numerically compared with those of four anatomical head models at different ages for 12 different mobile phone models (a total of 240 different configurations of mobile phones, head models, frequencies, positions, and sides of the head). The results demonstrate that the SAM phantom provides a conservative estimation of the SAR for only mobile phones with an antenna on top of the phone body and does not ensure such estimation for other types of phones, including those equipped with integrated antennas in the microphone position, which currently occupy the largest market share.

KEYWORDS
conservative estimation, electromagnetic field exposure, mobile phone, SAM phantom, SAR

1 | INTRODUCTION

Prior to being released in the market, mobile phones must be tested against electromagnetic field exposure limits. The International Commission on Non-Ionizing Radiation Protection (ICNIRP) Guidelines and IEEE standards define exposure limits in terms of a specific absorption rate (SAR) [1–3], and measurement techniques and procedures for determining the peak spatial-average SAR (psSAR) in the human head from radiation emitted from mobile phones used within close proximity to the ear are recommended in the International Electrotechnical Commission and IEEE standards [4,5]. The specific anthropomorphic mannequin (SAM) was designed and proposed as a standard head phantom.

One of the basic requirements for the standard phantom used in SAR compliance tests involves providing a conservative estimate of the SAR value. This means that the results assessed from the phantom should be higher than the expected exposure in the human head expected to occur under normal operational conditions. The SAM phantom (SAM for short, hereafter) has been implemented based on several studies on the dependence of the absorption by considering the anatomical structure, head size and shape, tissue parameters, and various types of phones [6–10]. Consequently, the shape and size of the SAM have been derived from a selected subset of the 90th percentile of US Army males [11].

Since then, many articles have reported that the SAM generally provides a conservative estimate of the peak spatial SAR averaged over a 1 or 10 g mass compared to human heads [12–17]. Most of these studies used phone models with an antenna source on top of the phone body in the form of a dipole, an external whip, an external helix, or an internal planar-inverted F antenna (PIFA), a generic phone with a monopole antenna on the metallic plane [12,13], a half-wavelength dipole antenna, a quarter-wavelength monopole antenna mounted over a metallic box, a PIFA built on the top part of a phone body [14], a generic phone and a PIFA built on the top part of a phone body [15,16], and three phone models equipped with an antenna on the top and two models equipped with an antenna at the bottom [17]. The latter two models of [17] are bar types, one of which has a flipped upside-down orientation of the top antenna model. For the flipped phone model with an antenna near the microphone, the SAM showed an underestimation of the 1 and 10 g psSARs at the cheek position.

Another study was recently conducted by researchers involved with the present paper [18]. Two bar phone models that operate in a dual band (835 and 1,850 MHz) were employed; one has the antenna at the bottom, and the other has it at the top. It was observed that the SAM clearly underestimates the 1 and 10 g psSARs when the phone operates at a higher frequency and the antenna is located at the bottom.

Based on extensive information regarding the commercial phone models available to the Korean market, a total of 11 typical phone models not including bar phone models with an antenna at the top have been numerically implemented [19]. These phone models are different in terms of their operating frequencies, outer shapes, and forms and locations of the antennae, and the number of commercial phone models corresponding to these types account for more than 86% of the total mobile phone models released in the market since 2002 (see Table 1).

The objective of this study was to generalize the results observed in [18] by expanding the types of numerical phone models. The phone models considered in this paper include bar, slider, and flip types operating at 835 MHz and 1,850 MHz (1,765 MHz for some flip-type models), which accurately reflect the characteristics of the physical sizes and the SAR distributions in the flat phantom of commercial phones [19]. The 1 and 10 g psSARs in four head models and the SAM are calculated and compared.

2 | PHONE MODELS AND METHOD

The 11 aforementioned mobile phone models were numerically implemented based on the SAR test reports and the phone manuals of commercial phone models released in the Korean market since 2002. The internal structures of each numerical phone model were designed such that the SAR values are similar to those of commercial phones in the corresponding category at the four standard positions i.e., left cheek, left tilt, right cheek, and right tilt against the SAM phantom. Therefore, the phone models described in this paper represent a significant number of commercial phones released over the past 15 years or so. Details of the numerical phone models are provided in [19].

For consistency in SAR comparison, the same anatomical head models with a $1 \times 1 \times 1$ mm^3 voxel size were used as those in [18]. The head models are from IT'IS, namely, Eartha (an 8-year-old female) and Louis (a 14-year-old male) of Virtual Classroom v. 1.0, and Billie (an 11-year-old female) and Duke (a 34-year-old male) of Virtual Family v. 1.0 [15].

A commercial electromagnetic simulation tool, SEMCAD X (2009) [20], with an FDTD solver was used for SAR calculation. After a three-dimensional SAR distribution of each

TABLE 1 Phone models

Numerical model	Market share (%)	Antenna type		Shape		Antenna location	Frequency (MHz)
M1	22.6	Internal (dual band)		Bar		Bottom	835 and 1,850
$M1_{rev}$	2.8			Bar		Top	
M2	8.8			Slider	Closed	Bottom	
M4					Open		
M3	15.0				Closed	Top[a]	
M5					Open		
M6	10.3			Flip		Bottom	
M7	4.9					Top[a]	835 and 1,765
M8w	10.7	External	Whip	Flip		Top (right)	835
M8h			Helix				835
M9w	14.1		Whip				1,765
M9h			Helix				1,765

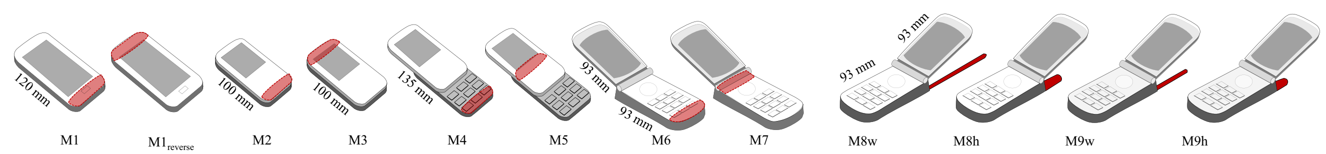

[a]The antenna is located at the top of the phone body in a closed state, and at the middle in an open state.

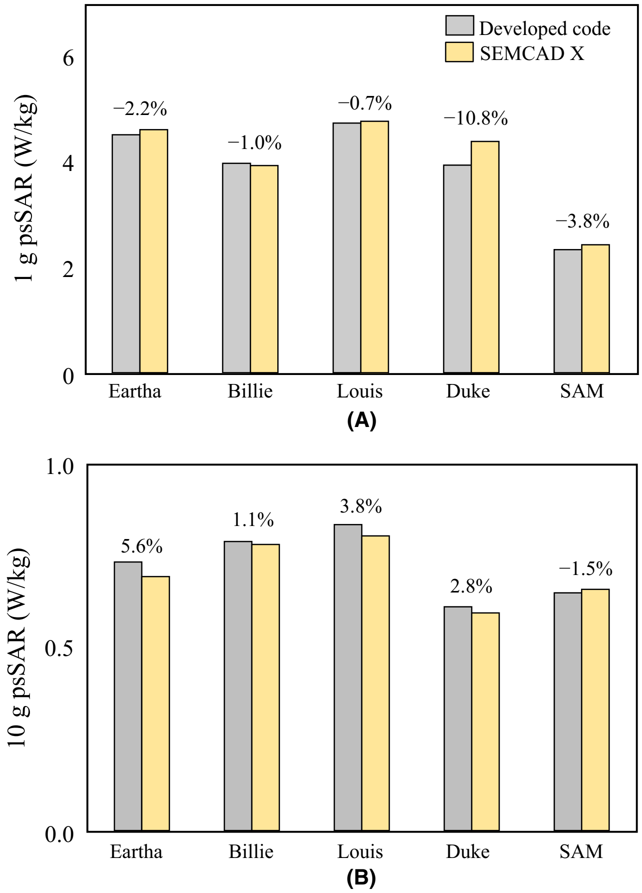

FIGURE 1 Comparison between psSAR values obtained using a developed code and commercial software, SEMCAD X (output power of 1.0 W): (A) 1 g psSAR at 1,850 MHz of M1 (cheek position) and (B) 10 g psSAR at 835 MHz of M1 (tilt position)

head model was exported from the solver with the same voxel size as the original head model, the SAR distribution was rotated backward toward the original upright head position to identify the head tissues. Then, the 1 and 10 g psSARs were determined using our own code according to IEEE C95.3 [21].

For code validation of the psSAR calculation, Figure 1 compares the psSARs calculated using our own code with those obtained by a commercial tool (SEMCAD X) for M1. The differences in their percentages are within approximately ± 10%. Both are based on the procedure of IEEE C95.3, and these differences can be caused by a few different aspects; for example, the exported SAR distribution has a different voxel size from the grid sizes, reconstructed for the SAR calculation in the commercial tool, and its direction in the rectangular coordinate system is different owing to the backward rotation from that of the commercial tool. However, these levels are under ± 30%, which indicates the uncertainty of the SAR measurement methodologies of international standards [4,5].

More than 1,400 test reports from 2002 to June 2013 were collected; 3% of the reports are about 40 phone models, and phone types accounting for less than 3% of the market share are likely to be unpopular. Therefore, the shape and dimensions of the phone body, as well as the antenna location and type for the numerical phone models, originated from phone types that account for over 3% of all SAR test reports of commercial phone models.

Table 1 presents 12 numerical phone types, which are the same as those in [22] with the exception of $M1_{rev}$. A bar-type phone model with an internal antenna on top of the phone is quite rare (2.8% market share, as shown in Table 1) in the Korean market, although such phones are common in European countries. This type of phone model, written as $M1_{rev}$ herein, was considered in [18] by simply rotating the original bar phone model positioned against a head phantom by 180° while maintaining its center, the results of which were integrated into this paper.

3 | SAR COMPARISON AND DISCUSSION

3.1 | Criteria on SAR conservativeness of SAM phantom

The psSAR of anatomical head models is compared with that of the SAM. The SAR ratio between the anatomical head models and the SAM is expressed by (1), which is the psSAR (1 or 10 g) expressed in decibels for the anatomical head models normalized to the SAM; a positive value indicates that the psSAR evaluated in an anatomical head model is larger than that in the SAM.

$$\text{SAR Ratio (dB)} = 10 \times \text{Log}_{10}\left(\frac{\text{psSAR}_{\text{Anatomical\_head}}}{\text{psSAR}_{\text{SAM\_phantom}}}\right). \quad (1)$$

An SAR calculation was basically conducted for the phone position on the right side of the head. However, for external antenna phone models, both the left and right sides were considered for a possible deviation in the psSAR when changing the test position from the right to the left side of the head, owing to their obvious one-sided feed point close to the right corner of the phone body.

At each frequency, the SAR was calculated for 120 configurations of the SAM or four anatomical head models, two positions, and right and left sides of the head. At 835 MHz, M1, $M1_{rev}$, M2, M3, M4, M5, M6, M7, M8w, and M8h from Table 1 were considered; 80 configurations (8 phone models × 2 positions × 5 head models × right side) for eight phone models with an internal antenna, and 40 configurations (2 phone models × 2 positions × 5 head models × 2 sides) for M8w and M8h with an external antenna, were used. At 1,765 MHz or 1,850 MHz, M1, $M1_{rev}$, M2, M3, M4, M5, M6, M7, M9w, and M9h were used for the SAR calculations.

This section presents the SAR ratio results for 1 and 10 g psSARs at 835 MHz and 1,765/1,850 MHz. The red and green bars in the graphs of Figures 2 and 5 indicate positive and

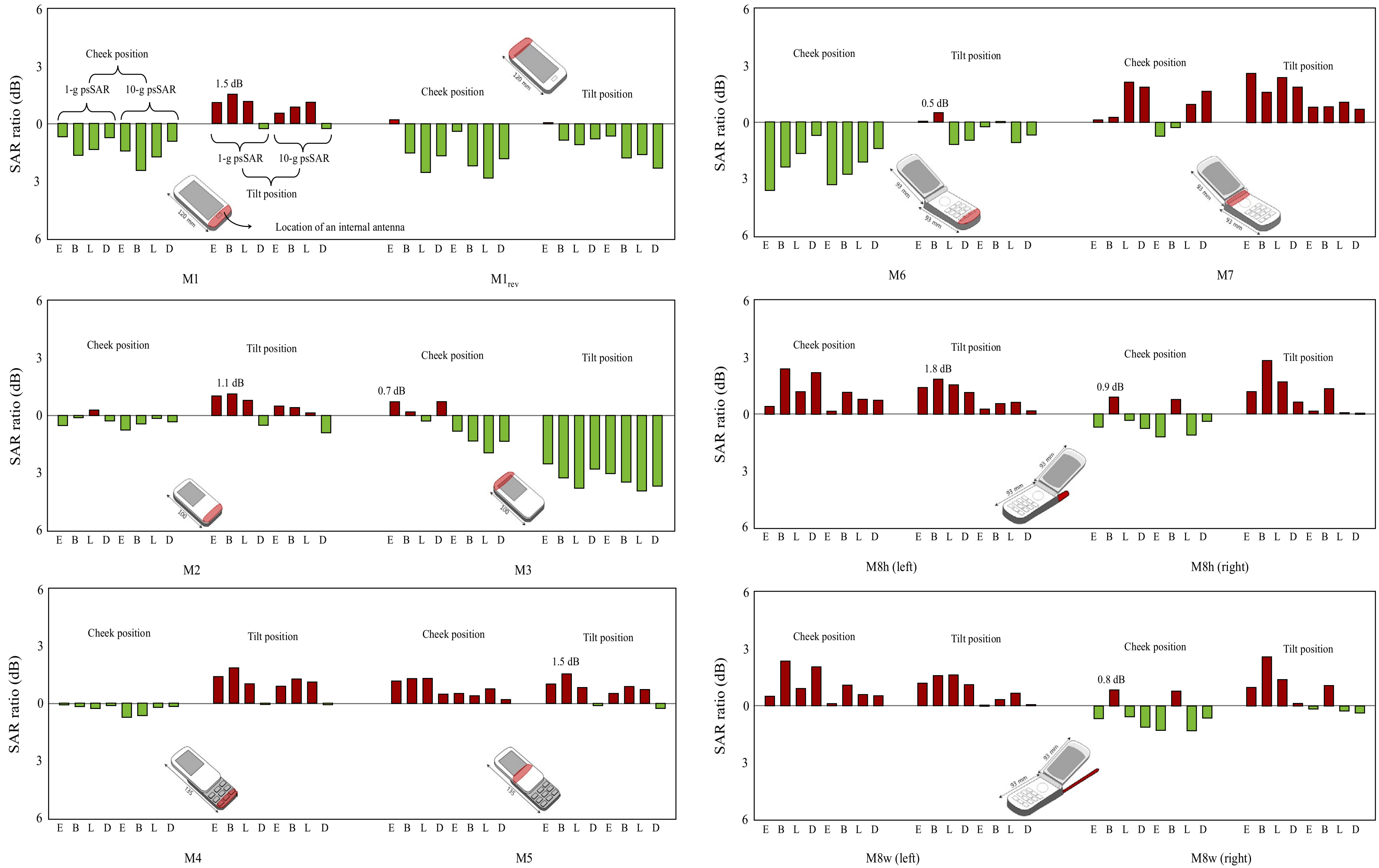

FIGURE 2 SAR ratio (835 MHz). The red part of the phones, from M1 to M7, indicates the internal antenna location, and helical and whip antennas are shown for M8h and M8w, respectively

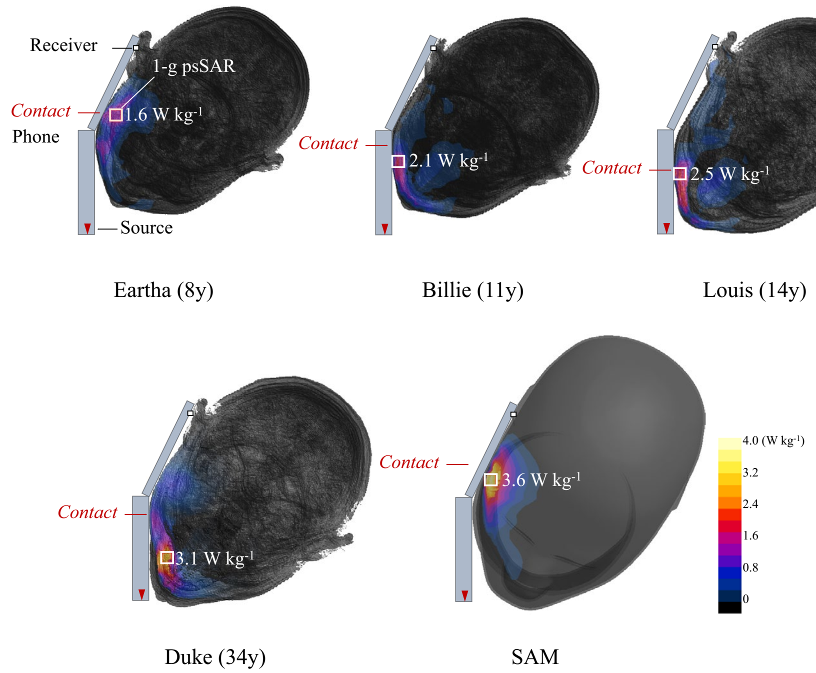

FIGURE 3 M6 and 1 g psSAR at 835 MHz (phone output power of 1.0 W)

negative ratio values, respectively, namely, ■ $psSAR_{Anatomical\_head} > psSAR_{SAM}$ and ■ $psSAR_{Anatomical\_head} < psSAR_{SAM}$. On the horizontal axis of the graphs, E, B, L, and D indicate Eartha, Billie, Louis, and Duke, respectively. For instance, the value of the bar for "E" represents the ratio (dB) of psSAR in the head model, Eartha, to that in the SAM. The graph of each phone model consists of 16 bars; the first eight bars are for the cheek position, and the remaining eight bars are for the tilt position. The corresponding numerical phone model is illustrated in each graph.

Commercial mobile phones should not exceed the 1 or 10 g SAR limits at both the cheek and tilt positions. According to international standards for measuring the psSAR of a mobile phone, a "conservative" estimate means that the measured value will not be less than the expected value during normal use by "a majority of users," including children using wireless communications devices [4,5]. However, the percentage of users that make up "a majority of users" is unclear.

Therefore, this paper proposes and applies the criteria of SAR conservativeness of the SAM; the SAM is considered

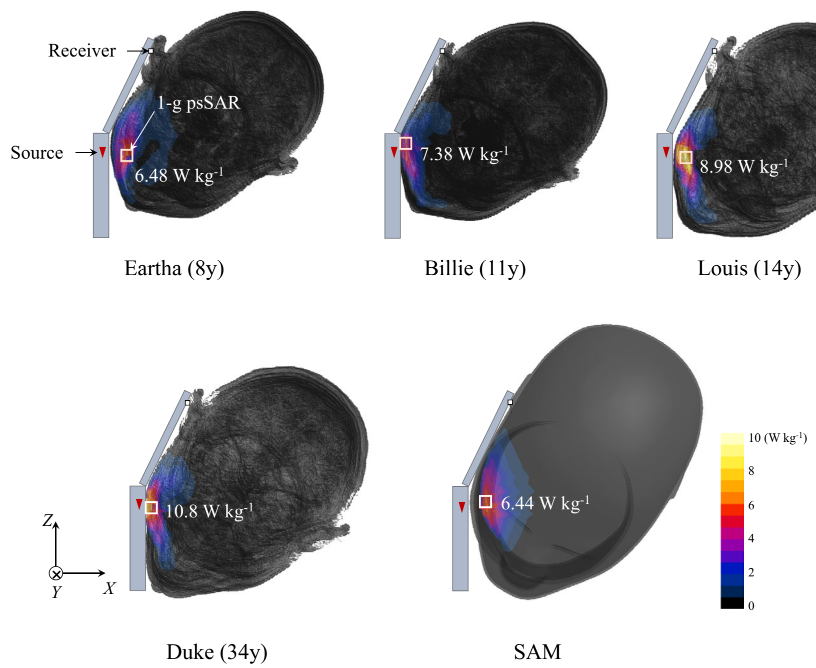

FIGURE 4 M7 and 1 g psSAR at 835 MHz (phone output power of 1.0 W)

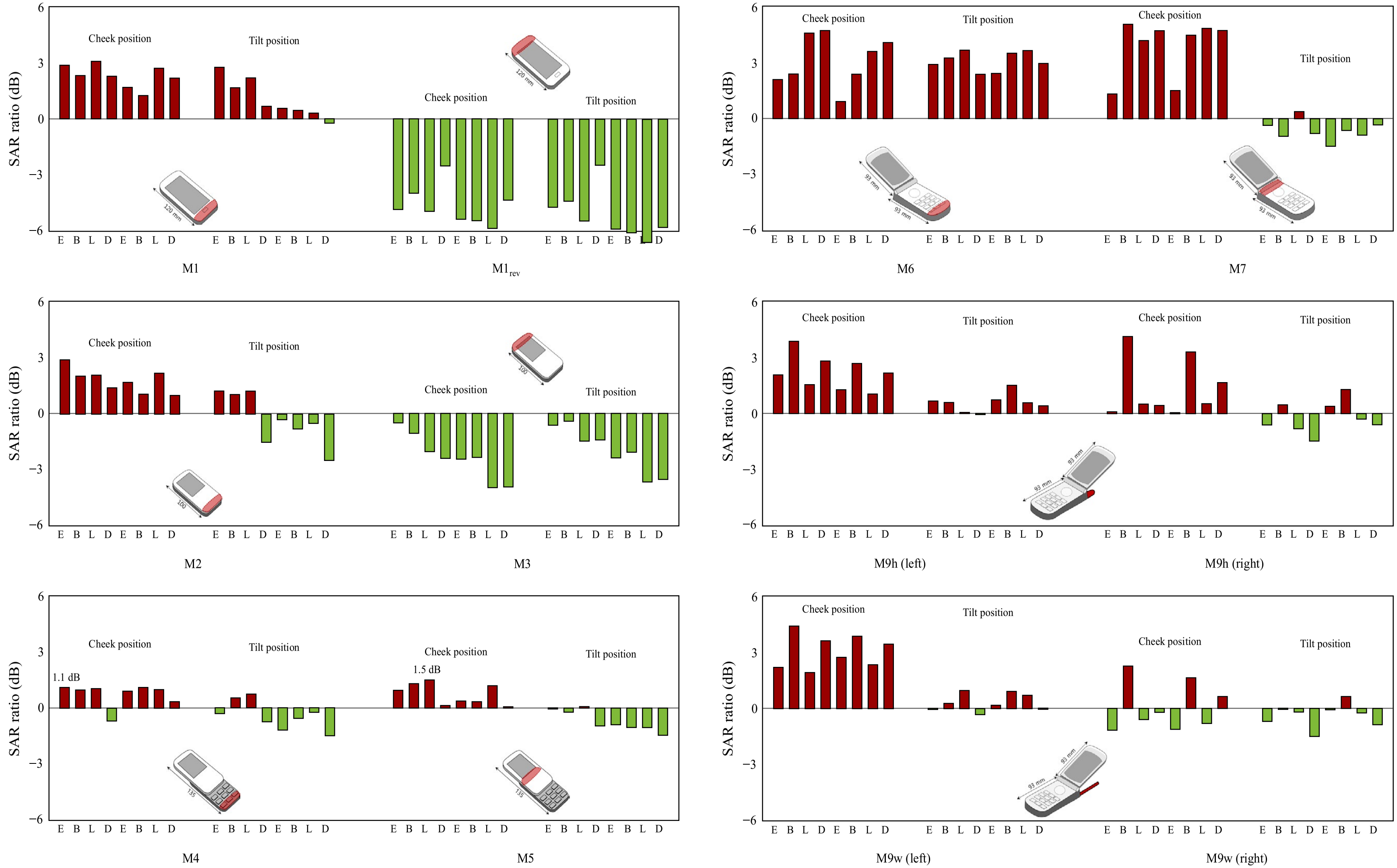

FIGURE 5 SAR ratio (1,765 MHz and 1,850 MHz). The red part of the phones from M1 to M7 indicates the internal antenna location, and helical and whip antennas are shown for M9h and M9w, respectively

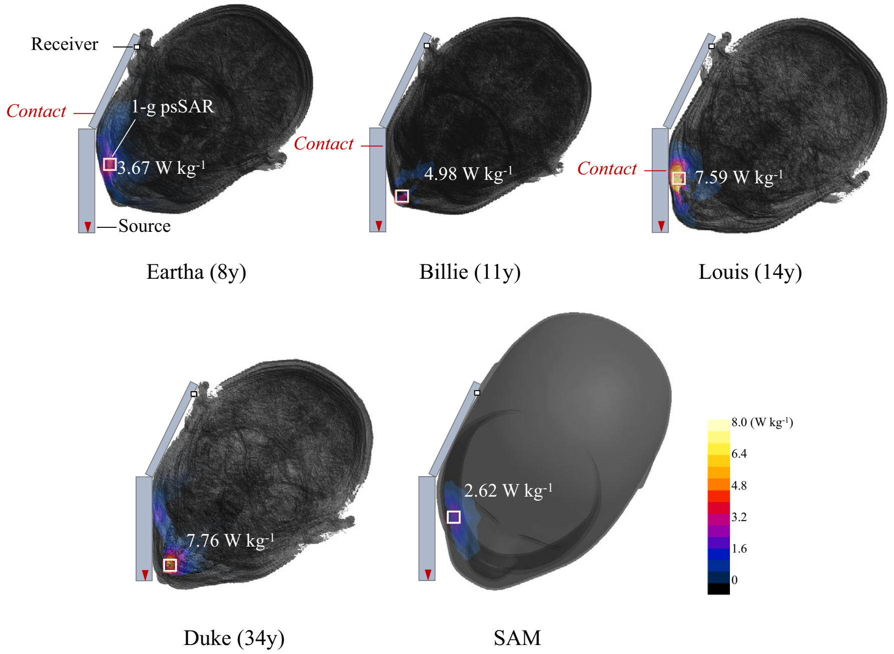

FIGURE 6 M6 and 1 g psSAR at 1,850 MHz (phone output power of 1.0 W)

conservative when one or both of the following conditions are satisfied.

(i) A negative SAR ratio is observed for more than two models of the four anatomical head models in both the cheek and tilt positions, and for the averaging masses of both 1 and 10 g. This implies that the SAM provides a higher psSAR than a majority of phone users.
(ii) For all configurations of a given phone model, any SAR ratio is lower than +1.1 dB, which means that the psSAR in an anatomical head is higher by about 30%. The 30% value is the same as the expanded measurement uncertainty of the SAR measurement methodologies developed in the international standards.

3.2 | 835 MHz

The 1 and 10 g psSARs of M1 are higher (negative values of SAR ratio) in the SAM than in the anatomical head models under the cheek position. However, under the tilt position, those in the

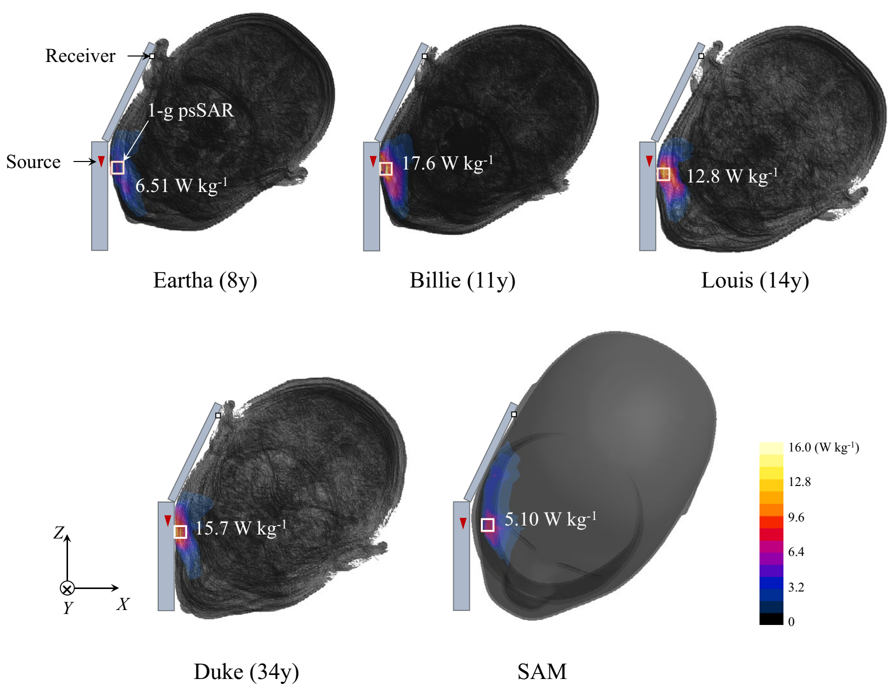

FIGURE 7 M7 and 1 g psSAR at 1765 MHz (phone output power of 1.0 W)

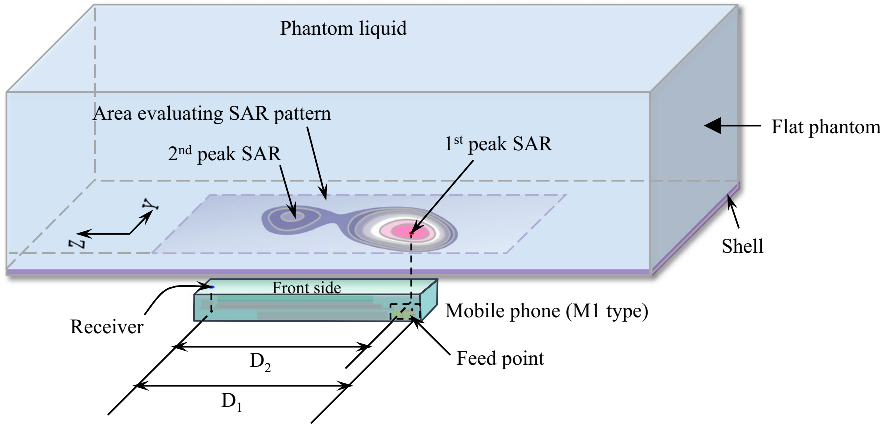

FIGURE 8 SAR pattern in the flat phantom (M1, 1,850 MHz).

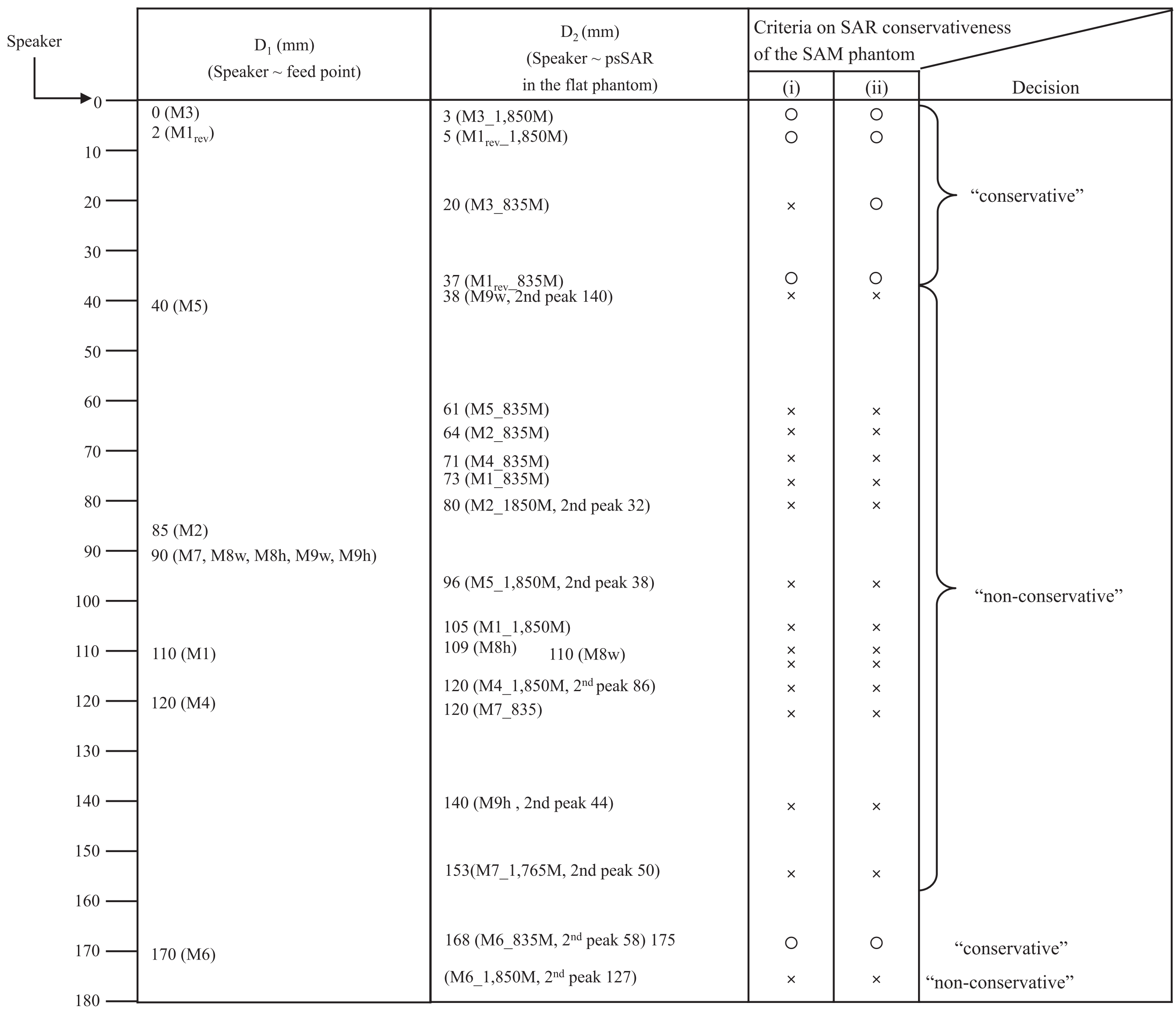

FIGURE 9 Antenna location of a mobile phone, psSAR location in the flat phantom, and conservativeness of SAM phantom

anatomical head models except Duke are higher, as shown in Figure 2. It was observed that the phone models with an internal antenna at the bottom such as M1, M2, and M4, demonstrate a similar trend in SAR ratios at 835 MHz; although the SAM provides a higher SAR at the cheek position, the SAM mostly exhibits a less SAR at the tilt position than the anatomical head heads.

For M3, a closed slider phone with an integrated antenna on the top, the psSAR values of Eartha, Billie, and Duke are higher than that of the SAM at the cheek position; however, their SAR ratios are less than +1.1 dB. Therefore, the SAM is considered conservative only for $M1_{rev}$, M3, and M6 at 835 MHz. Both $M1_{rev}$ and M3 commonly have an antenna at the top of the phone body.

The SAM is larger and has a thinner ear compared to the anatomical head models [4,5]. The contact point between a human head and a phone is dependent on the ear thickness and head shape. Figure 3 illustrates the contact point and the 1 g psSAR when M6 is held against the head models at the cheek position. The psSAR generally occurs around the contact point in many cases but can be changed based on the location of the source and the dielectric properties of the surrounding tissues. For M6 at 835 MHz, the "hotspot" (radiation-concentrated area) on the surface of an opened flip part will enlarge from the antenna to near the hinge of the flip, where most of the cheek of the head is very closely located. The flat cheek and the thin ear of the SAM make contact with the upper part of the flip phone and generate a higher psSAR than the anatomical heads.

Because all flip phone models have identical body dimensions, which are the average body dimensions of commercial flip phones, the contact points of the heads with M7 shown in Figure 4 are the same as those in Figure 3. The SAM is slightly farther from the phone source on the *x*-axis compared to Billie, Louis, and Duke, and thus the psSAR is lower than that in the anatomical head models.

Based on the above criteria (i) and (ii) for SAR conservativeness of the SAM, for a psSAR evaluation of M1, M2, and M4 at 835 MHz, the SAM is not considered conservative; three of the four anatomical head models demonstrate higher psSAR values at the tilt position, and the highest SAR ratio is greater than +1.1 dB for each phone model. Consequently, for all phone models, with the exception of $M1_{rev}$, M3, and M6, the SAM does not provide a conservative estimate of the psSAR at 835 MHz.

3.3 | 1,765 MHz and 1,850 MHz

In general, at this frequency, two hotspots of a smaller area than that at 835 MHz appear on the phone body because the wavelength is relatively short [19]. The stronger of the two hotspots occurs near the phone antenna. The 1 and 10 g psSAR ratios at 1,765 MHz and 1,850 MHz are shown in Figure 5. It was observed that the SAM provides a conservative estimate of the psSAR for $M1_{rev}$ and M3 at 1,850 MHz.

For M6, the SAM provided a higher psSAR than the anatomical head models at 835 MHz, but it produced a lower psSAR at 1,850 MHz, as shown in Figure 6. This can be attributed to different hotspot patterns and the SAR is weaker near the upper part of the flip part at 1,850 MHz [19]. For all head models, the psSAR of M7 occurred near the source and is lower in the SAM because the upper part of the flip phone touches the cheek of the SAM, and the lower part is farther from the SAM than from the anatomical head models, as shown in Figure 7.

The SAR level in a head model against a phone may be determined from a combination of the source location of the phone, the separation distance between the head and device, the operating frequency, and the tissue structure and properties near the hotspot. In conclusion, the SAM at 1,765 MHz and 1,850 MHz underestimates the psSAR of all phone models considered with the exception of $M1_{rev}$ and M3, which have the antenna at the top of the phone body, where the speaker is usually located.

4 | DISCUSSION

As shown in the previous section, the SAR ratio varies significantly between different phone designs and different head models because current flowing on a phone body is determined based on the design, operating frequency, and separation between the head and device.

SAR patterns were calculated in the flat phantom during the design process of numerical phone models [18]. Figure 8 presents an example of an SAR pattern at the flat phantom and at distances D_1 and D_2, which indicate the distance from the speaker to the antenna feed point and to the first peak SAR location of the SAR pattern, respectively, along the z-axis, parallel to the length of the phone body. The first and second columns of Figure 9 indicate D_1 and D_2 of the phone models considered. The first peak SAR indicates the maximum SAR calculated in the flat phantom.

The third column of the Figure 9 indicates whether the SAM underestimates the psSAR in the human head models according to criteria (i) and (ii) given in Section 3, namely, "○" when the criterion is satisfied, and "×" when not satisfied, which can be determined in Figures 2 and 5.

From the Figure 9, it can be observed that the SAM provides a conservative estimate of the psSAR (1 and 10 g) only when the feed point of a phone antenna is located close to the speaker, such as M3 and $M1_{rev}$, with the exception of M6 operating at 835 MHz. As stated earlier, it appears that M6 at 835 MHz created a larger hotspot because of a longer wavelength, and the flat contact area of the SAM around the upper part of the flip and the dielectric properties of the phantom liquid generated a higher psSAR than in anatomical heads. M3 and $M1_{rev}$ have an antenna at the top, and the psSAR occurred within about 40 mm from the speaker.

Phone designs, including the antenna, have evolved considerably since the standards for SAR compliance testing of mobile phones were first published during the early 2000s. For instance, mobile phones with an external antenna, usually on the top of the phone body, have completely disappeared. As mentioned in [19], many modern commercial mobile phones are of a bar type, where the main antenna for WCDMA, GSM, and LTE services is mostly located at the bottom of the phone body, although a few additional antennas supporting wireless local area networks, Bluetooth, and diversity reception are equipped at alternative locations inside the phone. The reason for such locations of the main antenna of commercial phones is because a phone with an antenna at the bottom generates a lower psSAR in the SAM than a phone with an antenna at the top. A longer bar phone with a bottom antenna, in this sense, would be more beneficial. The numerical phone model, M1, described in this paper represents the types of phones that currently occupy the largest market share.

5 | CONCLUSION

The SAM has been regarded to provide a conservative estimation of the actual psSAR of the electromagnetic field exposure radiating from a mobile phone. However, most related research results supporting the SAM have been based on early phone models, which have an antenna at the top of the phone body, as mentioned in Section 1.

Therefore, whether the SAM is sufficiently conservative has been numerically analyzed for various types of mobile phone models in this paper. The 1 and 10 g psSAR values in the SAM were compared with those in the four anatomical head models at different ages. The numerical phone models were selected and implemented based on an investigation of the SAR compliance test reports of commercial phone models that were released in Korea from 2002 to mid-2013. Each phone model was placed at the cheek and tilt positions on the right side of the head. The left-side exposure of the head was also considered for the phone models with an external antenna.

The results show that the SAM provides a conservative estimation of the SAR for mobile phones with an antenna at the top of the body but does not ensure such estimation for other types of phones, including those equipped with integrated antennas at the bottom of the phone body, that currently occupy the largest market share. As mentioned in our previous work [18], the underestimation of the SAR may be attributed to the geometrical relationship between the mobile phone and the SAM phantom and not the dielectric properties of the phantom liquid. Two important keys that the international standards have underlined in the design of the SAM phantom are the thin pinnae and large sized head. These must be modified to mitigate the shortcomings of the SAM phantom for the types of phones other than those with an antenna at the top.

REFERENCES

1. ICNIRP (International Commission on Non Ionizing Radiation Protection), *ICNIRP guidelines for limiting exposure to time-varying electric, magnetic and electromagnetic fields (up to 300 GHz)*, Health Phys. **74** (1998), 494–522.
2. IEEE Standard C95.1-2005, *IEEE standard for safety levels with respect to human exposure to radio frequency electromagnetic fields, 3 kHz to 300 GHz*, 2005.
3. IEEE Standard C95.1-1999, *IEEE standard for safety levels with respect to human exposure to radio frequency electromagnetic fields, 3 kHz to 300 GHz*, 1999.
4. Standard IEC62209-1, *Human exposure to radio frequency fields from hand-held and body-mounted wireless communication devices-human models, instrumentation, and procedures, Part 1: procedure to determine the Specific Absorption Rate (SAR) for hand-held devices used in close proximity to the ear (frequency range of 300 MHz to 3 GHz)*, Int. Electrotechnical Committee, Geneva, Switzerland, 2005.
5. IEEE Standard 1528-2013, *IEEE recommended practice for determining the peak spatial-average Specific Absorption Rate (SAR) in the human head from wireless communications devices: measurement techniques*, 2013.
6. V. Hombach et al., *The dependence of EM energy absorption upon human head modeling at 900 MHz*, IEEE Trans. Microw. Theory Tech. **44** (1996), 1865–1873.
7. K. Meier et al., *The dependence of electromagnetic energy absorption upon human head modeling at 1800 MHz*, IEEE Trans. Microw. Theory Tech. **45** (1997), no. 11, 2058–2062.
8. N. Kuster et al., *Dosimetric evaluation of handheld mobile communications equipment with known precision*, IEICE Trans. Commun. **E80-B** (1997), 645–652.
9. F. Schönborn et al., *The difference of EM energy absorption between adults and children*, Health Phys. **74** (1998), 160–168.
10. A. Drossos et al., *The dependence of electromagnetic energy absorption upon human head tissue composition in the frequency range of 300–3000 MHz*, IEEE Trans. Microw. Theory Tech. **48** (2000), 1988–1995.
11. C. G. Gordon et al., *1988 Anthropometric survey of U.S. army personnel: methods and summary statistics*, Technical Report NATICK/TR-89/044, U.S. Army Natick Research, Development and Engineering Center, Natick, Massachusetts, 1989.
12. W. Kainz et al., *Dosimetric comparison of the specific anthropomorphic mannequin to 14 anatomical head models using a novel definition for the mobile phone positioning*, Phys. Med. Biol. **50** (2005), 3423–3445.
13. B. B. Beard et al., *Comparisons of computed mobile phone induced SAR in the SAM phantom to that in anatomically correct models of the human head*, IEEE Trans. Electromagn. Compat. **48** (2006), 397–407.
14. V. Monebhurrun, *Conservativeness of the SAM phantom for the SAR evaluation in the child's head*, IEEE Trans. Magn. **46** (2010), 3477–3480.
15. A. Christ et al., *The virtual family—development of anatomical CAD models of two adults and two children for dosimetric simulations*, Phys. Med. Biol. **55** (2010), N23–N38.

16. A.-K. Lee et al., *A comparison of specific absorption rates in SAM phantom and child head models at 835 and 1900 MHz*, IEEE Trans. Electromagn. Compat. **53** (2011), 619–627.
17. J. Keshvari et al., *Large scale study on the variation of RF energy absorption in the head & brain regions of adults and children and evaluation of the SAM phantom conservativeness*, Phys. Med. Biol. **61** (2016), 2991–3008.
18. A.-K. Lee et al., *SAR comparison of SAM phantom and anatomical head models for a typical bar-type phone model*, IEEE Trans. Electromagn. Compat. **57** (2015), 1281–1284.
19. A.-K. Lee et al., *Numerical implementation of representative mobile phone models for epidemiological studies*, J. Electromagn. Eng. Sci. **16** (2016), 87–99.
20. SEMCAD X *Reference manual*, Schmid & Partner Engineering AG, Zurich, Switzerland, 2009.
21. IEEE Standard C95.3-2002, *IEEE Recommended Practice for Measurements and Computations of Radio Frequency Electromagnetic Fields With Respect to Human Exposure to Such Fields, 100 kHz-300 GHz*, 2002.
22. A.-K. Lee et al., *Mobile phone types and SAR characteristics of the human brain*, Phys. Med. Biol. **62** (2017), 2741–2761.

AUTHOR BIOGRAPHIES

Ae-Kyoung Lee received her BS and MS degrees in electronics and engineering from Chungang University, Seoul, Rep. of Korea in 1990 and 1992, respectively, and a PhD in radio science and engineering from Chungnam National University, Daejeon, Rep. of Korea in 2003. In 1992, she joined the Radio Technology Group at the Electronics and Telecommunications Research Institute, Daejeon, Rep. of Korea, where she has been involved in projects on measurement technologies and numerical analyses of electromagnetic compatibility and human exposure to RF fields. She was the recipient of the Japan Microwave Prize at the 1998 Asia-Pacific Microwave Conference, Japan and the Technology Award from the Korea Electromagnetic Engineering Society in 1999.

Seon-Eui Hong received her MS and PhD degrees in radio science and engineering from Chungnam National University, Daejeon, Rep. of Korea in 1999 and 2017, respectively. Since 1999, she has been with the Electronics and Telecommunications Research Institute, Daejeon, Rep of Korea, and is currently a principal member of the radio environment & monitoring research group. Her current research interests include numerical dosimetry and procedures for assessing an electromagnetic source.

Hyung-Do Choi received his MS and PhD degrees in material science from Korea University, Seoul, Rep. of Korea, in 1989 and 1996, respectively. Since 1997, he has been with the Electronics and Telecommunications Research Institute, Rep. of Korea. He has performed research on the biological effects of RF radiation and has developed RF radiation protection standards and regulations. His current research interests include spectrum management, microwave tomography, and EMC countermeasures.